Egyptian Journal of Petroleum xxx (xxxx) xxx

HOSTED BY

Contents lists available at ScienceDirect

Egyptian Journal of Petroleum

journal homepage: www.sciencedirect.com

Full Length Article

The polarographic and corrosion inhibition performance of some Schiff base compounds derived from 2-amino-3-hydroxypyridine in aqueous media

M. Abdallah [a,b,*], M. Alfakeer [c], H.M. Altass [a], Ahmed M. Alharbi [a], Isamil Althagafi [a], N.F. Hasan [b], E.M. Mabrouk [b]

[a] Chemistry Department, Faculty of Applied Science, Umm Al-Qura University, Makkah, Saudi Arabia
[b] Chemistry Department, Faculty of Science, Benha University, Benha, Egypt
[c] Chemistry Department, Faculty of Science, Princess Nourah bint Abdulrahman University, Riyadh, Saudi Arabia

ARTICLE INFO

Article history:
Received 31 July 2019
Revised 17 September 2019
Accepted 25 September 2019
Available online xxxx

Keywords:
Pyridine Schiff bases
Polarography
Corrosion inhibitor
Adsorption

ABSTRACT

The polarographic behavior of five Schiff bases compounds (SB) prepared from 2-amino-3-hydroxypyridine was investigated in BR buffer series of pH 2–12. The polarograms of all SB compounds displayed a single irreversible diffusion-controlled 2-electron wave within the whole pH range representing the saturation of the N=CH bond. The effect of pH and substituents on electrode reaction have been investigated and discussed. The electrode reaction pathway is found to be H^+, e, e, H^+ in which the proton uptake precedes the electron transfer. The studied compounds were used as inhibitors for corrosion of carbon steel (CS) in 1 M HCl solution using potentiodynamic polarization technique. The inhibition was explained in view of the adsorption of SP compounds on the CS surface obeying to Freundlich isotherm. These compounds act as good inhibitors as the inhibition efficiency reached 89.5%. The inhibition efficiency of the studied SBs is found to be a function of substituent group. The order of inhibition efficiency follows the sequence: N(CH3) > p-OCH3 > o-OH > H > p-Cl. This order agrees with the sequence of the negative shift in $E_{1/2}$ values of the SB compounds under investigation.

1. Introduction

Schiff bases (SB) which also known as azomethine are organic compounds analogues of ketones or aldehydes but the carbonyl group (C = O) is exchanged by an azomethine center (NH = C). They are used widely as ligands in coordination chemistry and preparation of metal complexes [1]. Recently SB compounds are used as catalysts in diverse biological systems and preparation of enzymes [2,3], as well as they also used in organic synthesis, medicine and pharmacy [4]. Schiff bases have important applications in hematopoietic systems [5], optical computers, preparation of acyclic and macrocyclic compounds, photodetectors in biological systems [6,7] and corrosion inhibitors [8–10]. Due to the thermal stability of these compounds they can be used as stationary phases in gas chromatography [11]. Moreover, electrochemistry of SB and their metal complexes was the subject of several studies [12–20] using polarography and cyclic voltammetry techniques.

Carbon steel (CS) is used in several industries, especially in the oil pipelines, chemical and electrochemical industries. Acidic solutions such as hydrochloric acid (HCl) are commonly applied for removing unwanted rust in many industrial operations but unfortunately, causes corrosion of CS. To solve this problem and reduce the rate of corrosion of CS in acid solutions, we use corrosion inhibitors which are mostly organic compounds that are easy to adsorb on the CS surface and diminish the rate of dissolution [21–30].

Although voltammetric studies of SB compounds were the subject of several investigations [31–36], little attention was paid to the electrochemical behavior of those derived from aminopyridine derivatives. The present study was conducted to follow the electrode reaction mechanistic pathway, evaluation of some electrochemical kinetic parameters and the use of the present pyridine SB to diminish the corrosion of CS in HCl solutions and deduced the correlation between the half-wave potentials and the inhibition efficiencies of these compounds.

Peer review under responsibility of Egyptian Petroleum Research Institute.

* Corresponding author at: Chemistry Department, Faculty of Applied Science, Umm Al-Qura University, Makkah, Saudi Arabia.
E-mail address: metwally555@yahoo.com (M. Abdallah).

https://doi.org/10.1016/j.ejpe.2019.09.002
1110-0621/

2. Experimental methods

2.1. Preparation of the solid SB compounds

The solid SB (I-V) were prepared by refluxing of an ethanolic solution of 2-mino-3-hydroxypyridine and benzaldehyde derivatives in 1:1 M ratio on a water bath for 4 hrs in presence of piperidene [32]. The resulting SB solid compounds that separated out on cooling and the mixture was filtered off, washed with ethanol, dried and recrystallized in ethanol. The benzaldehyde derivatives used were o-hydroxy benzaldehyde, p-chlorobenzaldehde, p-methoxybenzaldehyde and p-N-dimethyl benzaldehyde. The studied SB compounds have the following structural formulae shown in Scheme 1.

2.2. The elemental analysis, FT-IR and ^{1}H NMR of the SB compounds

Compound I: ^{1}HNMR (DMSO d_6), δ, ppm: 5.60 (s, 1H, OH combined to pyridine), 8.79 (s, 1H, CH of imine group), and 6.89–8.00 (m, 7H, CH of aromatic and pyridine rings)

IR, ν, cm-1, 3425 (OH stretching), 1614 (C = N stretching), 1570–1420 (C = C stretching of aromatic and pyridine rings), and 780–748 (CH out of plan bending of aromatic and pyridine rings).

Compound II: ^{1}HNMR (DMSO d_6), δ, ppm: 5 (s, 1H, OH combined to pyridine ring), 8.80 (s, 1H, CH of imine group), and 7–8.20 (m, 8H, CH of aromatic and pyridine rings)

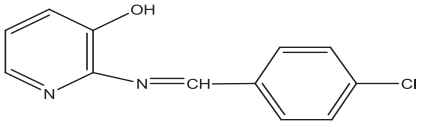

Compound I: 2-(4-chlorobenzylideneamino) pyridin-3-ol

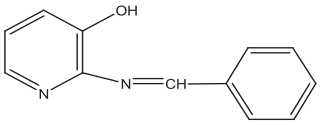

Compound II: 2-(benzylideneamino) pyridin-3-ol

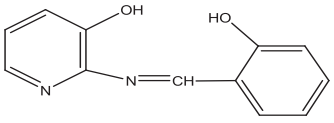

Compound III: 2-(2-hydroxybenzylideneamino) pyridin-3-ol

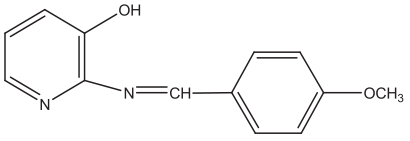

Compound IV: 2-(4-methoxybenzylideneamino) pyridin-3-ol

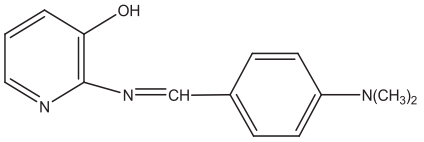

Compound V: 2-(4-(dimethylamino)benzylideneamino)pyridin-3-ol

Scheme 1. Structures of the prepared compounds.

IR, ν, cm-1, 3400 (OH stretching), 1600 (C = N stretching), 1550–1400 (C = C stretching of aromatic and pyridine rings), and 780–740 (CH out of plan bending of aromatic and pyridine rings).

Compound III: ^{1}HNMR (DMSO d_6), δ, ppm: 5.50 (s, 2H, OH combined to pyridine and aromatic rings), 8.83 (s, 1H, CH of imine group), and 7–8.20 (m, 7H, CH of aromatic and pyridine rings)

IR, ν, cm-1, 3420 (OH stretching), 1610 (C = N stretching), 1560–1410 (C = C stretching of aromatic and pyridine rings), and 785–743 (CH out of plan bending of aromatic and pyridine rings).

Compound IV: ^{1}HNMR (DMSO d_6), δ, ppm: 5.30 (s, 1H, OH combined to pyridine), 9.04 (s, 1H, CH of imine group), 4 (s, 3H, OCH_3 group), and 6.76–8.00 (m, 7H, CH of aromatic and pyridine rings)

IR, ν, cm-1, 3500 (OH stretching), 1622 (C = N stretching), 1575–1425 (C = C stretching of aromatic and pyridine rings), and 777–740 (CH out of plan bending of aromatic and pyridine rings).

Compound V: ^{1}HNMR (DMSO d_6), δ, ppm: 5.42 (s, 1H, OH combined to pyridine), 9.12 (s, 1H, CH of imine group), 3.41 (s, 6H, N $(CH_3)_2$ group), and 7.15–8.00 (m, 7H, CH of aromatic and pyridine rings)

IR, ν, cm-1, 3520 (OH stretching), 1618 (C = N stretching), 1575–1420 (C = C stretching of aromatic and pyridine rings), and 783–745 (CH out of plan bending of aromatic and pyridine rings).

2.3. Polarograhpic measurements

2.3.1. Preparation of SB solutions for polarographic measurements:

A stock solution (2 x 10^{-3} M) of each of the SB (I-V) was synthesized by dissolving the accurate weight of the solid compound in the convenient volume of ethanol. In the electrolysis cell, 1 mL of stock solution, 5 mL of Britton-Robinson (BR) buffer of the required pH and 4 mL of bi-distilled water were mixed to obtain 2x10^{-4} M of the depolarizer (SB) in 20% (v/v) as a final concentration. The electrolysis solution freed from dissolved oxygen was obtained by bubbling pure nitrogen gas followed by immediate scanning. The buffer solution used in the study was prepared following the standard procedure as recommended by Britton [36].

2.3.2. The polarographic cell

The used electrolysis cell consists of a dropping Hg capillary as a working electrode (WE), its characteristics are: rate of mercury falling (m) = 1.7 mg/sec, drop time (t) = 3.6 sec at a mercury height (h) = 60 cm and a saturated calomel electrode (SCE) as a reference electrode.

2.3.3. Estimation of the total number of electrons: Participated in the overall reduction process.

The complete number of electrons (n) is implicated in the overall reduction process was estimated experimentally using controlled potential electrolysis technique (coulometry) by using a digital coulometer model 179 from EG & G in which the electrolysis cell was a Hg pool cathode which a large surface area, the reference electrode was a SCE and the counter electrode was a Pt (CE).

2.3.4. Instruments

Average current–potential curves were registered by a pen recording Sargent-Welech polarograph model 4001. The registered polarograms were drawing by taking the middle of the oscillation after taking the necessary correction for residual current and sensitivity scale.

2.4. Corrosion measurements

2.4.1. Inhibitors solutions

A solution of 5 x 10^{-3} M of each of SB (I-V) were prepared by dissolving the exact weight of the SB in absolute ethanol. The required

Please cite this article as: M. Abdallah, M. Alfakeer, H. M. Altass et al., The polarographic and corrosion inhibition performance of some Schiff base compounds derived from 2-amino-3-hydroxypyridine in aqueous media, Egyptian Journal of Petroleum, https://doi.org/10.1016/j.ejpe.2019.09.002

concentration in the polarization cell was obtained by accurate dilution.

2.4.2. Chemical composition of CS electrode

The chemical composition of CS type L-52 has the following percentage (weight %) 0.26C, 1.35 Mn, 0.05Nb, 0.04P, 0.02 V, 0.03Ti and the remainder is Fe.

2.4.3. Potentiodynamic polarization (PDP) measurements

PDP measurements were accomplished in a three-electrode glass cell. The WE was CS L-52 of the above composition of 1 cm^2 area. A platinum foil of 1 cm^2 was used as CE, a SCE was utilized as reference electrode. The CS L-52 electrode was polished with some degree of emery papers, washed with bi-distilled water and degreased with acetone. The PDP measurements were accomplished using Mensberger Potentiostat /Galvanostat PS6 with a software PS remote. All the experiments were performed at scanning rate of 1 mV/sec. Each experiment was repeated at least three times and choose the high reproducibility. SD for the corrosion of current density was calculated.

3. Results and discussion

3.1. DC-Polarography

The dc-polarograms of SB compounds (I-V) were registered in Britton-Robinson (B.R) buffer series of pH 2–12 containing 20% (by volume) ethanol to insure the complete solubility of the SB compounds due to its incomplete solubility in pure aqueous media. Each polarogram consists of a single reduction wave within the entire pH range. The height of the polarographic wave (i_L) decreases gradually with rising the pH of the solution and the half-wave potential ($E_{1/2}$) shifts to more negative values revealing that both the $E_{1/2}$ and the limiting current (I_L) of the polarographic wave are pH-dependent and the hydrogen ions have participated in the reduction process and the proton uptake precedes the electron transfer [37]. A typical example of the investigated SB is represented in Fig. 1. The negative shift in $E_{1/2}$ is attributed to the decrease in the hydrogen ion concentration as the pH is increased. To discuss the gradual decrease of the limiting current ($i_{L)}$, the dissociation constant (pk_a) of the investigated Schiff base compounds were determined using potentiometric methods and found to be 7.2–7.8 according to the type of substituent in the compound. This gradual decrease in the wave height which occurs at pH corresponding to the pk_a value, describes that both forms in which the substance is present in the solution are imparted to the surface of electrode one of them, the protonated form (HA), is electroactive, and that the electroactive form can be generated from the electro-inactive one at a rate that depends on the pH [37]. This behavior may be due to an acid-base reaction since the wave height (i_L) still independent of pH if the formation of the acid form (active model) from the basic form (inactive model) is fast enough ($pH > pk_a$). As the pH increases ($pH < pk_a$), the rate of protonation decreases and consequently the wave height (i_L) decreases and a plot of the (i_L) against the pH is the shape of a dissociation curve (Fig. 2).

3.1.1. Investigation of the polarographic wave

The nature of the polarographic wave was investigated by performing the impact of Hg pressure (h) on the limiting current (i_l) and analysis of the polarographic wave. The effect of h on the limiting current (i_L) gives a straight line of a slope (*x*) applying the equation [38]: $\log i_L = \log k + \log h$. In the present study, the values of the slope (*x*) at some pH values (Table 1) ranging between 0.45 and 0.72, revealing that the electro- reduction process is fundamentally controlled by diffusion with some adsorption contribution. The thermodynamic reversibility of the electrode process was investigated from the logarithmic analysis of the polarographic wave [40]. The plots of E_{de} versus log $(i_d/i_d\text{-}i)$ at various pH values gave straight lines of slope S_1 (Table 1). From these slope values, the most probable values of the transfer coefficient (α) were determined and found between 0.31 and 0.58 at $n_a = 2.0$ (n_a the number of electrons involved in the rate-determining step). These results denoted that the electro-reduction process of all the SB compounds I-V happen irreversibly. The plots of $E_{1/2}$ versus pH are straight lines with slopes S_2. From the slope values S_1 and S_2 (Table 1), the number of hydrogen ions Z_H + involved in the rate-determining step was computed using the equation [39,40]:

$$dE_{1/2}/d(pH) = \left[(0.0951)Z_H^+\right]/\alpha n_a \quad (1)$$

The data obtained denotes that, the rate-determining step of the electrode reaction involves one proton and two electrons.

3.1.2. Effect of substituents

The influence of different substituents (X) in the p or m-position of the phenyl ring attached to the N = CH group on the half-wave potential of the polarographic waves of SB compounds I-V was inspected by applying the correlation Hammett equation [41]: $E_{1/2} = \rho_{\pi,R}\ \sigma_X$. The plots of $E_{1/2}$ versus Hammett substituent constants σ_x at pH 3 and 10 showed linear correlations (Fig. 3) of positive slopes ($\rho_{\pi,R}$) amounting to 0.1 and 0.12, respectively. The

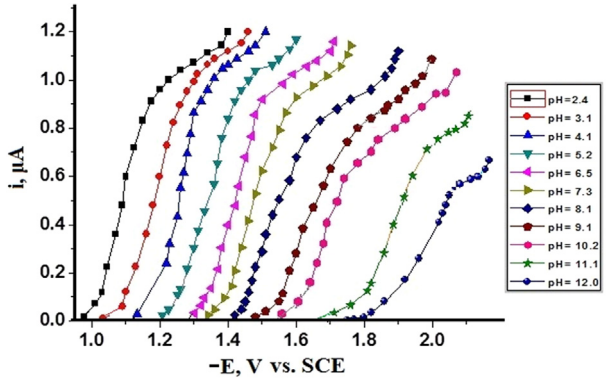

Fig. 1. DC-polarograms of compound V in various pH values.

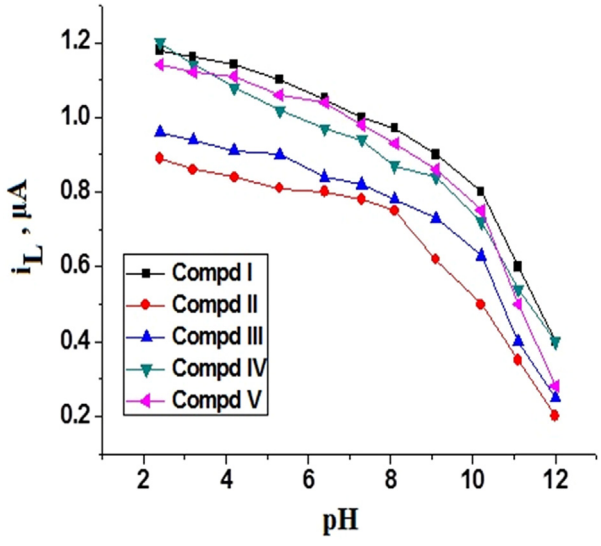

Fig. 2. i_L –pH plots for compounds I-V.

Please cite this article as: M. Abdallah, M. Alfakeer, H. M. Altass et al., The polarographic and corrosion inhibition performance of some Schiff base compounds derived from 2-amino-3-hydroxypyridine in aqueous media, Egyptian Journal of Petroleum, https://doi.org/10.1016/j.ejpe.2019.09.002

Table 1
DC-Polarographic data for SB compounds (I-V) in buffer solutions of various pH values.

Comp.	pH	i_l (μA)	$-E_{1/2}$ (V)	S_1 (mV)	α		S_2 (mV)	Z_H^+	δlogi/δlogh
					$n_a = 1$	$n_a = 2$			
I	3.2	1.18	0.93	80	0.73	0.37	50	0.62	0.60
	5.3	1.16	1.06	74	0.79	0.40	50	0.67	0.58
	7.3	1.00	1.12	68	0.85	0.43	50	0.73	0.60
	10.2	0.80	1.26	60	0.97	0.48	50	0.83	0.70
II	3.2	0.89	1.10	51	1.15	0.58	60	1.17	0.45
	5.3	0.81	1.25	62	0.94	0.47	60	0.96	0.55
	7.3	0.78	1.36	51	1.15	0.58	60	1.17	0.65
	10.2	0.50	1.51	64	0.91	0.46	60	0.93	0.79
III	3.2	0.96	1.01	74	0.79	0.40	50	0.67	0.40
	5.3	0.90	1.25	83	0.70	0.35	50	0.60	0.45
	7.3	0.82	1.**36**	80	0.73	0.37	50	0.62	0.50
	10.2	0.63	1.48	90	0.64	0.32	50	0.55	0.55
IV	3.2	1.20	1.07	95	0.62	0.31	70	0.74	0.55
	5.3	1.02	1.22	95	0.62	0.31	70	0.74	0.45
	7.3	0.94	1.37	105	0.56	0.53	70	0.63	0.40
	10.2	0.72	1.50	111	0.53	0.56	70	0.66	0.40
V	3.2	1.14	1.12	83	0.70	0.35	70	0.84	0.50
	5.3	1.06	1.30	74	0.79	0.37	70	0.94	0.60
	7.3	0.98	1.37	80	0.73	0.40	70	0.87	0.65
	10.2	0.75	1.58	95	0.61	0.31	70	0.73	0.72

$S_1 = 0.0591/\alpha n_a$ $S_2 = \delta E_{1/2}/\text{pH}$ $Z_{H+} = S_2/S$.

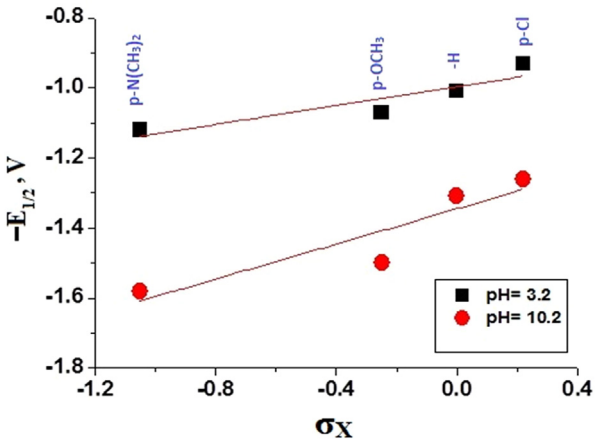

Fig. 3. $E_{1/2}$ - σ_x plots for SB compounds I-V.

values of (σ) were taken from the tabulation of Ritchie and Sager [42]. The general trend obtained is the negative shift of the $E_{1/2}$ of the electron-donating substituents required higher energy. On the other hand, electron-withdrawing substituents facilitate the electrode reaction and hence lower energy is required.

3.1.3. Estimation of the total number of electrons

In order to suggest the pathway of reaction mechanism, the total number of electrons participates in the reduction process (n) should be estimated. This was achieved by using controlled potential electrolysis (coulometry), the total number of electrons involved in the electro-reduction process was calculated experimentally in buffer solution of pH 3. In this technique, the potential of the mercury pool-working electrode was adjusted at the limiting current value of the polarographic wave (plateau). The background current of the buffer is firstly measured and cancelled, then the appropriate concentration ($1x10^{-4}$ M) of the compound (SB) is placed into the electrolysis cell and the electrolysis is continued to completion. The amount of charge, Q, in coulombs is measured directly from the digital coulometer. The total number of electrons (n) involved in the electro-reduction process is calculated using the equation: $Q = nFW/M$, in which W is the weight of the SB in grams and M its molecular weight. The measurements were made in buffer solutions of pH 3 and 9 for all SB compounds I-V and the data obtained are given in Table 2.

3.1.4. Electrode reaction mechanism

According to Zuman [38], if the polarograms have a single polarographic wave, it may behave in any three ways; (i) neither the half-wave potential nor the limiting current changes as the pH changes, (ii) the half-wane potential is pH dependent whereas the limiting current is pH-independent, (iii) both the half-wave potential and the limiting current are pH-dependent, this may be due to that the two forms in which the substance in solution are transferred to the electrode vicinity, thus one of them is electroactive and that the electroactive form is generated from the electro-inactive one and the pH controls this generation, which is the present case. In this case, the wave height still constant if the formation of the active form from the inactive one is fast enough. On increasing the pH, the protonation rate decreases and consequently the wave height (i_L) decreases as well and a plot of the limiting current (i_L) as a function of pH is a dissociation curve (Fig. 2). The general sequence of the electrode reaction is H^+, e, H^+, e or H^+, e, e, H^+ in which the proton uptake precedes the electron transfer. Based on this assumption and the behaviour of i_L – pH and $E_{1/2}$ – pH plots and the data obtained from controlled potential electrolysis, the mechanism of the reduction process may be suggested as represented in Scheme 2.

3.2. SB compounds as corrosion inhibitor

3.2.1. Potentiodynamic polarization curves

Fig. 4 shows the PDP curves of the tested CS L-52 electrode in 1.0 M HCl solution in the absence and presence of some concentrations ($1x10^{-5}$-$1x10^{-3}$ M) of compound V as a typical example for SB compounds at 25 °C. Inspection of Fig. 4 reveals that the inhibitor shifts the anodic curves into the positive direction and the cathodic curves towards the negative direction. This behavior suggested the inhibiting effect of the additives. The various electrochemical parameters such as the anodic Tafel slopes (β_a) and the cathodic Tafel slopes (β_c), the corrosion potential (E_{corr}), the corrosion current density (i_{corr}), the inhibition efficiency (IE) and the surface coverage (θ) were computed and given in Table 3. The percentage

Please cite this article as: M. Abdallah, M. Alfakeer, H. M. Altass et al., The polarographic and corrosion inhibition performance of some Schiff base compounds derived from 2-amino-3-hydroxypyridine in aqueous media, Egyptian Journal of Petroleum, https://doi.org/10.1016/j.ejpe.2019.09.002

Table 2
Controlled potential electrolysis (Coulometry) of SB compounds (I-V) at different pH values.

Comp.	Mol. Wt. g mol^{-1}	pH	Applied potential (V)	Weight of sample (g) $\times 10^{-4}$	Number of coulombs	Total number of electrons
I	198	3.2	− 1.10	1.98	0.0950	1.95 ≈ 2
II	214	3.2	− 1.15	2.14	0.0848	1.88 ≈ 2
III	232	3.2	− 1.10	2.32	0.0851	2.05 ≈ 2
IV	228	3.2	− 1.25	2.28	0.0813	1.92 ≈ 2
V	241	3.2	− 1.35	2.41	0.0713	1.78 ≈ 2

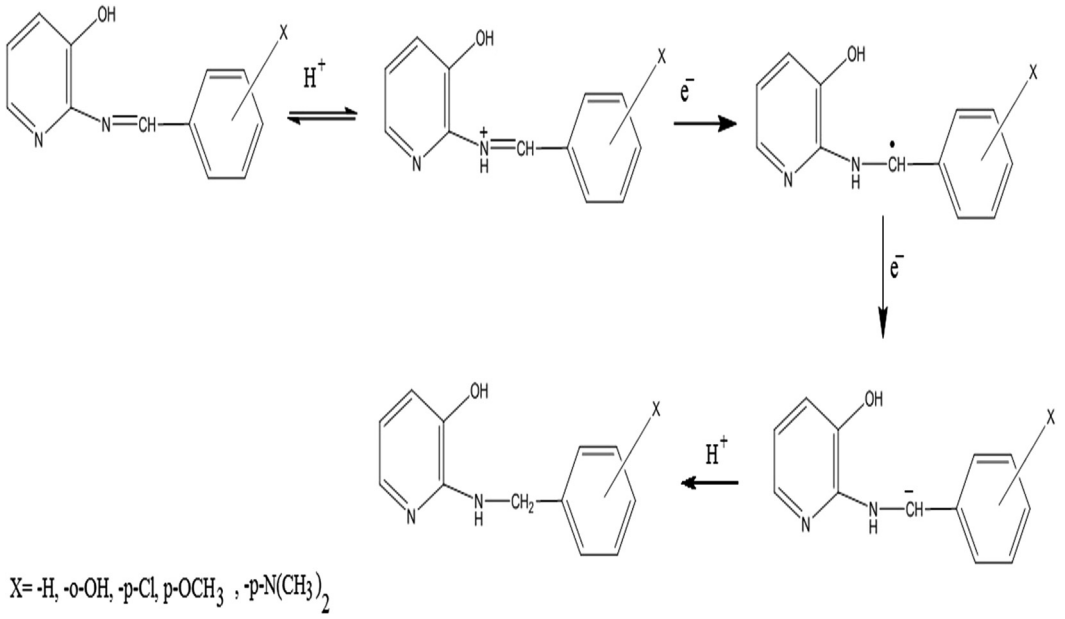

Scheme 2. Mechanism of the electrode reaction.

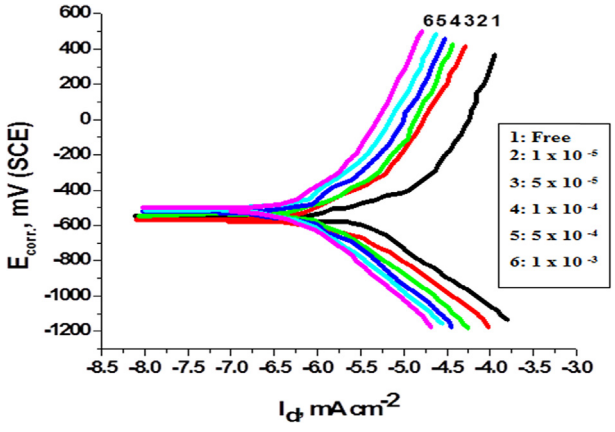

Fig. 4. PDP curves of CS L-52 electrode in 1.0 M HCl solution without and with various concentrations of compound V.

inhibition efficiency (% IE) of the used SB compounds was calculated using the next equation:

$$\%\,IE = (i - -i_{add}/i_{free}) \times 100 \quad (2)$$

where, i_{add}, i_{free} are the corrosion current densities in the presence and absence of the SB compounds, respectively.

It is evident from Table3 that, the increase of the concentration of SB compounds (I-V) led to the values of β_c and β_c are changed slightly which signalizes that SB acted as mixed type inhibitors i.e. reduce the anodic dissolution of CS and retard the cathodic hydrogen evolution reaction [43]. $E_{corr.}$ is a little shifted in the active direction in comparison to the result obtained in the absence of the SB compounds the values of I_{corr} decrease in all the studied concentrations, and the values of % IE increases proving the inhibiting impact of SB compounds. The values of % IE decreases in the subsequent sequence:

Comp. V > Comp. IV > Comp. III > Comp. II > Comp. I

These compounds that have been studied are more efficient inhibition than reported in the literature [44,45].

3.2.2. Adsorption isotherm

SB compounds (I-V) like organic molecules inhibit the corrosion of CS in HCl solutions by its adsorption on the CS surface. The adsorption operation can be considered as replacement process in which an inhibitor molecule, SB, in the aqueous phase substitutes an "z" number of water molecules adsorbed on the CS surface as follows:

$$SB_{(aq)} + z\,H_2O_{(sur)} \rightarrow SB_{(sur)} + z\,H_2O_{(aq)} \quad (3)$$

where z is defined as size ratio and equals the number of adsorbed water molecules interchange by a single inhibitor molecule. The adsorption process depends on several factors such as the chemical structure of additives the presence substituents (donating or repelling groups), the position of the metal in the periodic table, temperature and others. Trials were performed to fit the surface coverage (θ) values to some adsorption isotherms to select the appropriate isotherm. To a large extent, the results were better processed by applying the Freundlich isothermal equation [46,47]:

$$\log\theta = \log K + n \log C \quad (4)$$

Please cite this article as: M. Abdallah, M. Alfakeer, H. M. Altass et al., The polarographic and corrosion inhibition performance of some Schiff base compounds derived from 2-amino-3-hydroxypyridine in aqueous media, Egyptian Journal of Petroleum, https://doi.org/10.1016/j.ejpe.2019.09.002

Table 3
The effect of increasing concentrations of SB compounds on the corrosion parameters obtained from PDP measurement for CS corrosion in 1.0 M HCl solution at 25 °C.

IE%	θ	β_c mV dec.$^{-1}$	β_a mV dec.$^{-1}$	$I^{-2}_{corr.}$ μ A cm	$E_{corr.}$- mV(SCE)	Conc., M	System
–	–	155	170	0.324 ± 0.005	522	0.0	Blank
53.70	0.537	154	172	0.150 ± 0.001	526	1×10^{-5}	Comp. I
58.02	0.580	148	162	0.136 ± 0.003	528	5×10^{-5}	
61.42	0.614	143	173	0.125 ± 0.001	527	1×10^{-4}	
71.60	0.716	135	169	0.092 ± 0.002	512	5×10^{-4}	
75.62	0.756	132	160	0.079 ± 0.001	505	1×10^{-3}	
59.26	0.593	154	169	0.132 ± 0.003	524	1×10^{-5}	Comp. II
62.96	0.629	148	166	0.120 ± 0.002	520	5×10^{-5}	
68.52	0.685	142	165	0.102 ± 0.001	518	1×10^{-4}	
76.54	0.765	140	160	0.076 ± 0.001	514	5×10^{-4}	
80.86	0.809	136	158	0.062 ± 0.001	508	1×10^{-3}	
63.58	0.636	150	170	0.118 ± 0.002	516	1×10^{-5}	Comp. III
69.75	0.697	146	168	0.098 ± 0.001	520	5×10^{-5}	
73.45	0.734	140	160	0.086 ± 0.001	551	1×10^{-4}	
80.24	0.802	138	164	0.064 ± 0.001	512	5×10^{-4}	
83.95	0.839	132	160	0.052 ± 0.001	504	1×10^{-3}	
68.52	0.685	148	168	0.102 ± 0.002	525	1×10^{-5}	Comp. IV
72.84	0.728	144	164	0.088 ± 0.001	520	5×10^{-5}	
77.16	0.772	138	160	0.074 ± 0.001	516	1×10^{-4}	
83.33	0.833	136	158	0.054 ± 0.0007	510	5×10^{-4}	
86.11	0.861	130	164	0.045 ± 0.0005	502	1×10^{-3}	
72.22	0.722	152	170	0.090 ± 0.001	528	1×10^{-5}	Comp. V
76.54	0.765	150	174	0.076 ± 0.0006	540	5×10^{-5}	
81.86	0.819	142	166	0.062 ± 0.0005	526	1×10^{-4}	
85.18	0.852	138	160	0.048 ± 0.0003	512	5×10^{-4}	
89.50	0.895	135	156	0.034 ± 0.0001	495	1×10^{-3}	

in which C is the concentration of the SB compounds and K is the equilibrium constant of the adsorption. Fig. 5 symbolizes the plot of log θ against log C. A straight line is gained with intercept equal to log K. These resulted indicates that the adsorption of SB (I-V) on the surface of CS L-52 follows Freundlich adsorption isotherm.

The equilibrium constant of adsorption (K_{eq}) is associated to the standard free energy of adsorption ΔG^o by the relation:

$$K_{eq} = 1/55.5\ exp\ (-\Delta G^o_{ads}/\ RT) \quad (5)$$

in which R is gas constant and 55.5 is the molar concentration of water. The values of K equal to 53.7, 56.2, 60.2, 66.0 and 70.7x10^{-2} for compounds I, II, III, IV and V, respectively. The values of ΔG^o were calculated and found equal to −21.99, −24.09, −27.75, −33.23 and −38.14 kJ mol^{-1} for SB I, II, III, IV and V, respectively. The values of ΔG^o_{ads} decreases in the following sequence:

Comp. V > Comp. IV > Comp. III > Comp. II > Comp. I.which is coincided with the values of % IE. The negative values of ΔG^o_{ads} donate that the adsorption of the studied SB compounds on the surface of CSL-52 is spontaneous process.

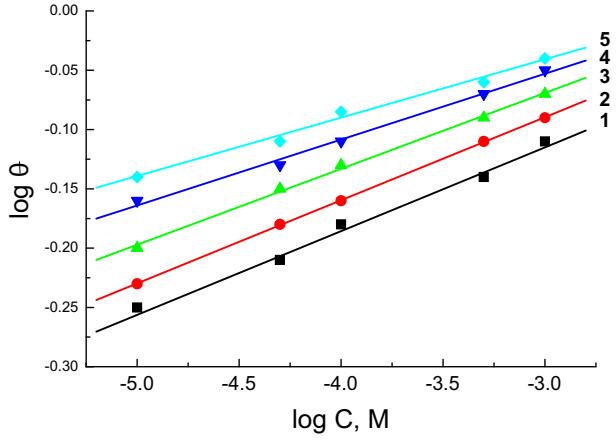

Fig. 5. Relation between log θ against log C according to Freundlich isotherm.

3.2.3. Mechanism of inhibition

It's well known that the inhibiting effect of organic molecules containing hetro atoms is due to the formation of bond between the metal and the lone pair of electrons in the additive [48]. The inhibiting impact of the tested SB compounds is due to the adsorption of the inhibitor molecules at the CS/solution interface, thus corrosion inhibition can be interpreted in terms of adsorption advantages [49].

The inhibitory strength of SB compounds toward the corrosion of CS in 1 M HCl solution can be demonstrated by the formation of the complex between ferrous ion and CS compound as shown in Scheme 3. This complex is adsorbed on the CS surface, and thereby isolating the steel from the corroding acid attack.

To give more light on the mechanism of interaction between the Schiff bases and steel surface, the $E_{1/2}$ values were plotted versus the inhibition efficiency values of testing SB compounds (Fig. 6). It is clear that the increase in %IE follows the order: N $(CH_3)_2$ > OCH_3 > OH > H > Cl

This order is satisfactory agreed with the data obtained from polarography in which the $E_{1/2}$ values shifted to more negative side in the same direction. This may be ascribed that the negative shift in $E_{1/2}$ increases the stability of these compounds to electro-reduction. The electron-donating substituents (p-OCH_3, p-N $(CH_3)_2$) increases the electron density at the C = NH center leading

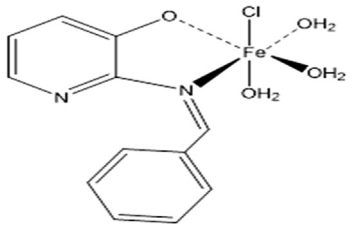

Scheme 3. The complex formed between CS and SB.

Please cite this article as: M. Abdallah, M. Alfakeer, H. M. Altass et al., The polarographic and corrosion inhibition performance of some Schiff base compounds derived from 2-amino-3-hydroxypyridine in aqueous media, Egyptian Journal of Petroleum, https://doi.org/10.1016/j.ejpe.2019.09.002

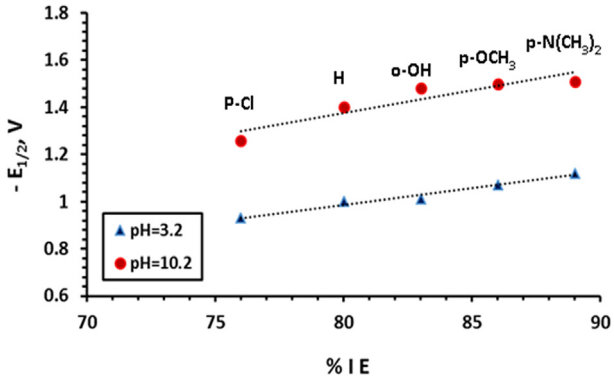

Fig. 6. The plot of $E_{1/2}$ and %IE for the SB compounds(I-V).

to increasing the attraction between inhibitor molecule and metal surface, thus inhibition efficiency is increased.

4. Conclusion

1- SB compounds were reduced via a single 2-electron, irreversible diffusion-controlled polarographic wave comparable to the saturation of the azomethine center.
2- The influence of substituents on the electrode reaction was inspected.
3- SB compounds were utilized as corrosion inhibitors for CS in 1MHCl solutions using PDP measurements.
4- PDP proved that the SB compounds acted as mixed inhibitor.
5- The inhibition efficiency depending on the concentration of SB compounds and the presence of the functional groups in the additives.
6- The inhibitory action on SB was interpreted by the formation of a complex between CS and SB adsorbed on the steel surface.
7- The adsorption follows Freundlich isotherm.

Acknowledgment

This research was funded by the Deanship of Scientific Research at Princess Nourah bint Abdulrahman University through the Fast-track Research Funding Program.

References

[1] P. Souza, J.A. Garcia-Vazquez, J.R. Masaguer, Trans. Met. Chem. 10 (1985) 410–412.
[2] H. Naaeimi, J. Safari, A. Heidarnezhud, Dyes and Pigments 73 (2007) 251–253.
[3] S. Kumar, D.N. Dhur, P.N. Saxena, J. Sci. Ind. Rev. 68 (2009) 181–187.
[4] K.K. Upadhyay, A. KumarS, P.C. Mishra Upahyay, J. Mol. Struct. 873 (2008) 5–16.
[5] M. Ozastan, I.D. Karagox, I.M. Kilic, M.E. Guldev, J. Biotechnol. 10 (2011) 2375–2387.
[6] K. Tanaka, R. Shimoura, M.R. Tetrahedron lett., 51(2010) 449-452.
[7] G. Pistolis, D. Gegiou, E. Hadjoudis, J. Photochem. Photobiol. A. Chem. 93 (2–3) (1996) 179–184.
[8] E.E. Elemike, D.C. Onwudiwe, H.U. Nwankwo, E.C. Hosten, J. Mol. Struct. 1136 (2017) 253–262.
[9] A. Yurt, H. Dal, Appli. Surf. Sci. 253 (2006) 919–925.
[10] H. Ashassi-Sorkhabi, B. Shabani, B. Aligholipour, D. Seifzadeh, Appli. Surf. Sci. 252 (2006) 4039–4047.
[11] A.M. Attia, N.O. Shaker, N.E. Maysour, Prog. Org. Coat 129 (2006) 985–998.
[12] Bao-Xian Ye, Xu. Yan, Fei Wang, Fu. Yong, Mao-Ping Song, Inorg. Chem. Commun. 8 (2005) 44–47.
[13] A.A. Isse, A. Gennaro, E. Vianello, Electrochim. Acta 42 (1997) 13–14.
[14] J. Pineda, M. Blazquez, M. Desminguez, F. Garcia-Blance, J. Electroanal. Chem., Interfac. 294 (2010) 178–192.
[15] S. Zolzzi, E. Spodine, A. Decini, Polyhyd. 21 (2002) 55–59.
[16] A.K. Gupta, R.S. Sindal, J. Chem. Sci. 121 (2009) 347–351.
[17] H.A. Kianfar, H.M.M. Abadi, R.H. Fath, M. Roushhani, Inorg. Chem. Resear. 1 (2016) 9–20.
[18] A. Djedouanl, H. Bendaas, A. Mousser, Acta Crystallo., A 63 (2007) 231–234.
[19] T. Balic, B. Markovi, M. Medavidovic-Kosanvic, J. Mol. Struct. 1084 (2015) 82–88.
[20] R. Benramdane, F. Benghanem, A. Ourari, G. Bouet, J. Coordination Chem., 68 (2015)560-572.
[21] A. Fawzy, M. Abdallah, M. Alfakeer, H.M. Ali., Int. J. Electrochem. Sci. 14 (2019) 2063–2084.
[22] M. Ahmed El Defrawy, Jabir Al-Fahemi Abdallah, J. Mol. Liq. 288 (2019) 110994.
[23] M. Abdallah, M.A. Hegazy, M. Alfakeer, H. Ahmed, Green Chem. Lett. Rev. 11 (2018) 457–468.
[24] R.S. Abdel Hameed, M. Abdallah, Prot. Met. Phys. Chem. Surf., 54(2018)113-121.
[25] S Abdel Hameed, Adham El-Zomrawy, M. Abdallah, S. S. Abed El Rehim, H.I. AlShafey, Nour Edin Shaher, Int. J. Corro. Scale Inib., 6(2017)196-208.
[26] M. Abdallah, Hatem M. Altass, B.A. AL Jahdaly, M.M. Salem, Green Chem. Lett. Rev. 11(2018)189-196.
[27] R.S. Abdel Hameed, M. Alfakeer, M. Abdallah, Surf. Eng. Appl. Electrochem. 54 (2018) 599–606.
[28] M. Abdallah, M. Alfakeer, N.F. Hasan, Ahmed M. Alharbi, E.M. Mabrouk, Orient J. Chem. 35 (2019) 98–109.
[29] M. Abdallah, E.A.M. Gad, M. Sobhi, Jabir H Al-Fahemi, M.M. Alfakeer, J. Egypt, Petroleum 28 (2019) 173–181.
[30] M. Abdallah, H.M. Al –Tass, B.A.AL Jahdaly, A.S. Fouda, J. Mol. Liq. 216 (2016) 590-597.
[31] M.M. Ghoneim, E.M. Mabrouk, A.M. Hassanein, M.A. El-Attar, E.A. Hesham, Cent. Europ. J. Chem. 5 (2007) 898–911.
[32] I.S. El-hallag, G.B. El-Hefnawy, Y.I. Moharram, E.M. Ghoneim, Can. J. Chem. 75 (2000) 1170–1177.
[33] A.A. Isse, A. Gennaro, E. Vianello, Electrochim. Acta 42 (1997) 2065–2071.
[34] J.M. Sevilla, G. Cambron, T. Pineda, M. Blazquez, J. Electroanal. Chem. 381 (1995) 179–183.
[35] T. Pineda, M. Blazquez, M. Dominguez, F. Garciablanco, J. Electroanal. Chem. 294 (1990) 179–192.
[36] H.T.S. Britton, Hydrogen Ions, 4th Ed., Chapman and Hall, London, 1952, p. 364.
[37] P. Zuman, The Elucidation of Organic Electrode Process, Academic Press, New York, 1969.
[38] J. Heyrovesky, J. Kuta, Principles of Polarography, Pubilishing House of the Czech Acad. Sci. (1965) 61.
[39] L. Meites, Polarographic Techniques, Interscience Publishers Inc., 4th Ed., New York, 1955
[40] M.M. Ghoneim, M.A. Ashy, Can. J. Chem. 57 (1979) 1294–1298.
[41] H.P. Hammett, Physical Organic Chemistry, McGraw-Hill, New York, 1940.
[42] C.R. Ritchie, W.F. Sager, Progress in Physical Organic Chemistry, Vol. 2, Interscience Publishers Inc. (1964) 334.
[43] R. Sayed Abdelwahed, M. Saleh, M.A. Al-Omair, H.M. Abd Al-Lateef, J. Mol. Str. 184 (2019) 452–461.
[44] A.M. Eldesoky, M.M. Ghoneim, M.A. Diab, A.A. El-Bindary, A.Z. El-Sonbati, M.K. Abd El-Kader, J. Mater. Environ. Sci. 6 (2015) 3066–3085.
[45] L.H. Madkour, U.A. Zinhome, J. Corros, Sci. Eng. 13 (2010) 1–28.
[46] F.M. Al- Nowaiser, M. Abdallah, E.H. El-Mossalamy, Chem. Tech Fuels Oils 47 (2012) 453–463.
[47] M. Abdallah, I.A. Zaafarany, S. Abd El Wanees, R. Assi, Int. J. Electrochem Sci 9 (2014) 1071–1086.
[48] M. Abdallah, Sh. T. Atwa, M. Abdallah, I.M. El-Naggar, A.S. Fouda, Anti Corros. Meth. Mater. 58 (2011) 31-38
[49] M.M. Saleh, Manal G. Mahmoud, Hany M. Abd El-Lateef, Corros. Sci. 154 (2019) 70–79.

Please cite this article as: M. Abdallah, M. Alfakeer, H. M. Altass et al., The polarographic and corrosion inhibition performance of some Schiff base compounds derived from 2-amino-3-hydroxypyridine in aqueous media, Egyptian Journal of Petroleum, https://doi.org/10.1016/j.ejpe.2019.09.002